International Journal of
Turbomachinery
Propulsion and Power

MDPI

Article

Contamination of Brush Seals by Oil and Salt and Its Impact on Rubbing and Hysteresis Behaviour

Manuel Hildebrandt, Corina Schwitzke * and Hans-Jörg Bauer

Institute of Thermal Turbomachinery (ITS), Karlsruhe Institute of Technology, Kaiserstraße 12, 76131 Karlsruhe, Germany; manuel.hildebrandt@kit.edu (M.H.); hans-joerg.bauer@kit.edu (H.-J.B.)
* Correspondence: corina.schwitzke@kit.edu; Tel.: +49-721-608-44182

Received: 11 September 2019; Accepted: 6 December 2019; Published: 11 December 2019

Abstract: The literature already contains some experimental, analytical and numerical investigations on the rubbing and hysteresis behaviour of brush seals. What the investigations have in common is that they were carried out with new and uncontaminated seals, or that such a condition was assumed. The influence of contamination has not been explicitly investigated yet. Particularly in stationary gas and steam turbines, foreign substances can accumulate on and in the bristle package during steady-state operation. In the case of a rubbing event with a contaminated brush seal, e.g., during shutdown of the machine, the process is not expected to be comparable to that assumed in the presence of a new, uncontaminated seal. The present paper is dedicated to the question of the influence of contamination on the total frictional power loss generated during rubbing and the distribution of heat fluxes in friction contact. For this purpose, rub tests with two seals were carried out on the brush seal test rig of the Institute of Thermal Turbomachinery (ITS) in new conditions. Subsequently, the sealing packages were contaminated with oil or a salt mixture. After the treatment, the rub tests were repeated and compared with the previous tests. In addition, stiffness measurements were used to assess the degree of contamination. A strong influence on the rubbing behaviour by the contamination was detected. Contamination causes the flexibility of the bristle package to be greatly reduced. As a result, especially at the beginning of the first measurements, the total power losses and rotor heat inputs are strongly increased. This flexibility is partly regained in the course of the measurements. As expected, contamination also influences the hysteresis behaviour of the seal. A highly increased leakage rate after rubbing could be observed, because the bristles remained close to their deflected positions. In the case of the salted seal, however, an improvement in the leakage performance could be observed after several repeat tests.

Keywords: brush seal; contamination; frictional heat input; rotor heat input; heat flux distribution; hysteresis

1. Introduction

Brush seals have been applied in turbomachinery for over 30 years and have become a real alternative to labyrinth seals. This type of seal is intended for use in almost every new aircraft engine and is also mounted in land-based turbomachinery or retrofitted in existing plants.

The research and development of brush seals began with rig tests, mostly at a component level, focusing on the leakage and wear properties of the seal. Later, the seal was installed and tested in test engines and finally it was widely used in the field. Over the years, a large amount of information has been gathered on the long-term behaviour of brush seals as part of maintenance work and regular checks on the condition of the seals. Publications [1–6] provide examples of this in extracts. The focus in assessing the seals was primarily on the wear condition and the change in leakage rates over time.

For understanding the operating behaviour of the seal and the conclusions that can be drawn from this for the design process, however, the temperature increases and heat input during rubbing of the seal against the rotor are also of great importance. Previous experimental and theoretical investigations on this topic have been carried out with new seals, or such a state has been assumed (see: [7–14]). In order to design brush seals for a long service life and an extended range of applications, the degree of wear and contamination must also be taken into account. If the bristle package is contaminated during operation, for example, as a result of a polluted medium (poor steam quality [15,16]) or as a result of oil coking [17], its properties change and the rubbing and leakage behaviour is no longer comparable to the behaviour in the new condition.

In the studies published so far, the influence of the degree of contamination has been insufficiently investigated. In certain publications, only photographs of the seals are shown, which qualitatively illustrate the degree of contamination that can occur after a longer period of use [18–20]. Only Pastrana et al. [15] describe further investigations and results on this topic. They report on experiments in which sodium chloride (NaCl) or potassium chloride (KCl) deposits were formed by immersing brush seal samples in water solutions of sodium chloride and potassium chloride—in various concentrations—then boiling off the water. In static measurements they could determine a reduction of the leakage rates in the case of contamination due to a reduction of the seal porosity as well as a substantial increase in the package stiffness. The latter, however, only lasts until the deposits are either broken by force (in which case the stiffness recovers to within 2.5× its original value) or the deposits are washed off. Within the scope of dynamic tests, the influence of NaCl deposits on heat generation was investigated. First, a measurement without contamination was carried out. The seal was mounted with a 0.254 mm interference on a 129.5 mm diameter rotor. The speed was 4000 rpm (27.13 m/s) and kept constant for one hour. After 10 minutes, a steady-state temperature at the seal/rotor junction of 34 °C was measured with thermal imaging equipment. After completion of the tests, the seal was removed and immersed in a 5 % solution of NaCl and then baked at 482 °C for one week. By repeating the experiments, a temperature of 108 °C at the seal/rotor junction, higher by a factor of 3.17, could be measured after 3.5 minutes. Within 20 minutes, however, a steady-state temperature of approximately 40 °C was reached again.

In this paper, similarly to Pastrana et al. [15], direct comparisons are carried out between contaminated and unpolluted seals. A salt solution and turbine oil were selected as media to contaminate the seal packages. While Pastrana et al. [15] determined the influence of contamination and its change over time with one test over several minutes, specific repeat measurements under constant conditions were carried out within the scope of this investigation. The measurements thus represent the case of a seal which has been continuously contaminated over a long period of operation and then repeatedly rubs against a rotor within a shorter period of time. Repeat measurements allow the influence on the hysteresis behaviour to be investigated more precisely by comparing the leakage rates between the runs. In addition, a focus is placed not only on the temperatures in friction contact, but also on the total power loss and distribution of the heat fluxes into the rotor and seal. A better understanding of how the degree of contamination of a brush seal influences its properties with regard to leakage, heat input and wear will offer the potential to improve the efficiency and power yield of turbomachinery in the future.

2. Materials and Methods

2.1. Brush Seal Test Rig

The test rig at the Institute of Thermal Turbomachinery (ITS) (see Figure 1) is a rotating test rig allowing for seal examinations under machine-oriented operating conditions. It is based on the test rig described in [7,8]. The target parameters of the tests on this test rig are the leakage mass flow and the heat fluxes while the seal is rubbed on the rotor. The experiments can be carried out at maximum pressure differences across the seal of up to 9 bar, circumferential velocities of up to 280 m/s

and rotor–seal interferences of up to 0.5 mm. The interference can be adjusted both eccentrically and concentrically. The test rig is operated with air at ambient temperature and is driven by an electric three-phase asynchronous motor. Between the driving motor and the rotor bearing, a torque transducer is installed. The rotor disk consists of Inconel 718 and has a diameter of 299.5 mm on the right front edge (see Figure 1). The rotor is instrumented with thermocouples embedded in the rotor structure very close to the rub surface. The telemetry unit, which is directly attached to the rotor, is used to transfer the temperature data of thermocouples to the static system.

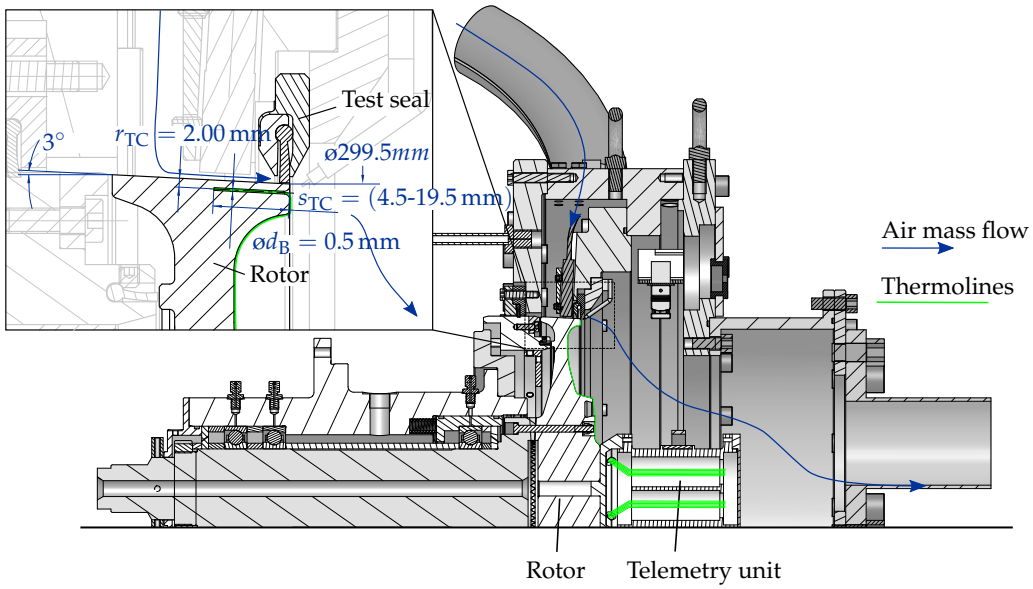

Figure 1. Sectional view of test rig. Detail: Bore hole geometry of rotor instrumentation.

As mentioned above, one of the target parameters is the leakage mass flow through the tested seal. The mass flow measurement is carried out by several differential pressure metering orifices according to DIN EN ISO 5167 with nominal diameters of 32, 80 and 100 mm. Depending on the flow, the implemented control automatically switches between the three different orifices. In this way, all relevant mass flows between 6 and 584 g/s can be measured within an accuracy of ±1.5 %. A number of parameters is commonly available for assessing the leakage behaviour of sealing systems. In this paper, the discharge coefficient c_d was used. This value is defined by the ratio of the measured leakage flow through the seal to an idealized, inviscid gap flow:

$$c_d = \frac{\dot{m}_{bs}}{\dot{m}_{ideal}}. \tag{1}$$

The gap flow is defined by an isentropic nozzle flow, which is represented by the following equation:

$$\dot{m}_{ideal} = A \cdot p_{t,in} \cdot \sqrt{\frac{2 \cdot \kappa}{R \cdot T_{t,in} \cdot (\kappa - 1)}} \cdot \sqrt{\left(\frac{p_{out}}{p_{t,in}}\right)^{\frac{2}{\kappa}} - \left(\frac{p_{out}}{p_{t,in}}\right)^{\frac{(\kappa+1)}{\kappa}}}. \tag{2}$$

A is the annular gap area between the back plate and the rotor. The leakage flows of the static and secondary axial brush seals are not measured.

The other target parameters are the heat flows while rubbing. Concentric rubbing of the seal is realised by moving the housing and therefore the seal in the axial direction to the left along the conically shaped rotor. The cone angle of the rubbing surface is 3.0°. The rotor was instrumented with the primary objective of measuring the friction-related, transient rotor temperatures during the rubbing of the brush seal against the counter-surface. For this purpose, an in situ measurement of

temperatures using thermocouples embedded in the rotor structure close to the rubbing surface was installed. A total of 24 (4×6) thermocouples of type *K* with a diameter of 0.5 mm are inserted into bore holes at a distance of 2.0 mm parallel to the rotor surface. The temperatures are measured at 11 different axial positions. The axial distance between the thermocouples is 1 to 2 mm. For redundancy, the temperatures of each axial position are measured at two circumferential positions displaced by 180°. At the axial measuring position of 7.5 mm away from the right rotor edge, four thermocouples are arranged circumferentially at 90° intervals for a better estimation of the temperature distribution along the circumference. To increase the heat conduction between the rotor structure and the thermocouples, the bore holes are filled with a heat-conductive paste with a thermal conductivity of 3.8 $\mathrm{W/(m\,K)}$.

2.2. Evaluation Method

Based on the measured transient temperatures, however, it is not possible to readily deduce the desired heat input into the rotor structure. Since the assumption of a thermally thin body is not valid in this case, both the local and the temporal temperature gradients must be taken into account. Moreover, the geometry of the experimental set-up is too complex to solve the problem by applying analytical equations. For this reason, a numerical model for finite element analysis was chosen.

The numerical model was built as a two-dimensional, axisymmetric model representing the rotor and a part of the shaft. The modelled parts are shown in Figure 2. All non-symmetrical areas of the rotor, in particular the screw connection to the shaft, were assumed not to be influenced thermally during the 30 s of rubbing. They were nevertheless modelled to correctly calculate the displacements of the rubbing surface due to rotational forces. To justify the simplification of a 2D model, a comparison with a 3D model was made. A mesh independency study was also carried out. The model was set up as a thermomechanically coupled model to calculate both the mechanical and thermal deformations. This is necessary because the value of the set interference was corrected with the value of the thermal and mechanical expansion during rubbing. The convective heat transfer was considered along the dashed line shown in Figure 2. Convective heat transfer coefficients were calculated with analytical correlations according to [21]. On all non-marked surfaces, adiabatic conditions were assumed. The heat input itself was specified as a boundary condition in the model. It was iteratively varied until there was a satisfactory agreement between the temperatures of the experiment and numerical simulation. In doing so, the temperature sensors, which are located closer to the heat input surface, were weighted more strongly in the correction procedure of the heat input. The white points highlighted in Figure 2 represent the temperature measurement locations in the experiment. In order to quantify the influence of the external boundary conditions and the bore tolerances on the temperature measurement as well as the subsequent calculation of the heat input, a sensitivity analysis was carried out. The results of this analysis are summarized in [22].

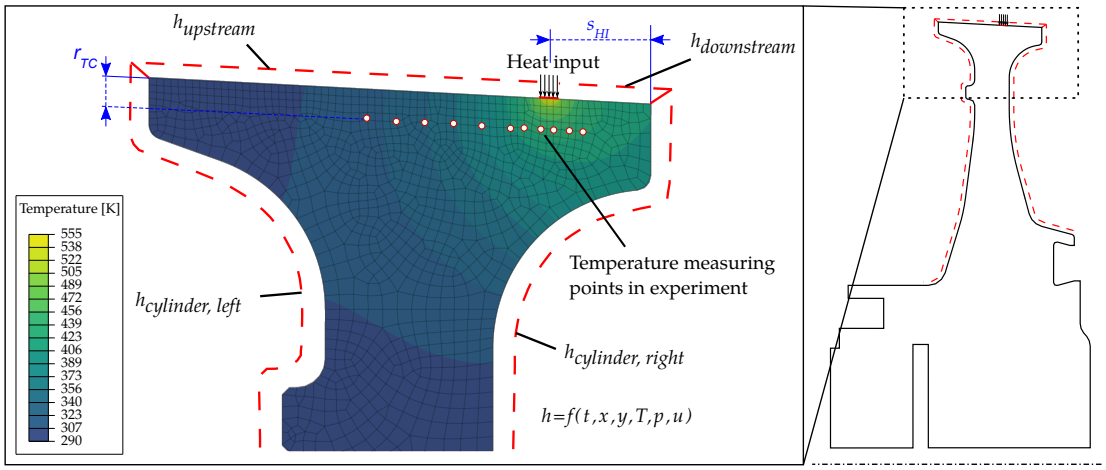

Figure 2. Two-dimensional finite element model [7].

2.3. Investigated Seals

The experimental results discussed in this paper are based on two clamped-type seals. The geometry parameters are listed in Table 1. Since both seals were contaminated with different substances and differ in axial distance between the bristle package and the back plate s_{ax}, a direct comparison between the seals is not intended. Instead, the respective measurements of the individual seals before and after contamination are compared with each other.

Table 1. Seal parameters.

Parameter		Seal O(il)	Seal S(alt)
seal inner diameter d_s	(mm)	300	
laying angle λ	(°)	45	
bristle diameter d_b	(mm)	0.10	
packing density ρ_p	(Bpmm)	140	
back plate inner diameter		Identical	
nominal bristle pack width b	(mm)	2.97	
bristles material		Haynes 25	
ax. dist. package to back plate s_{ax}	(mm)	0.00	0.63
Contamination medium		Turbine oil	Salt mixture

2.3.1. Treatment of Contaminated Seals

In the following, the specific treatments of seals *O* and *S* for the following investigations will be described in more detail. The seals were not in a new condition before the treatment, but had already been rubbed against an Inconel 718 rotor 75 times (seal *O*) or 28 times (seal *S*) under different operating conditions. These tests include those used for later comparison with the measurements in the contaminated state. The initial conditions are shown in Figure 3a,b.

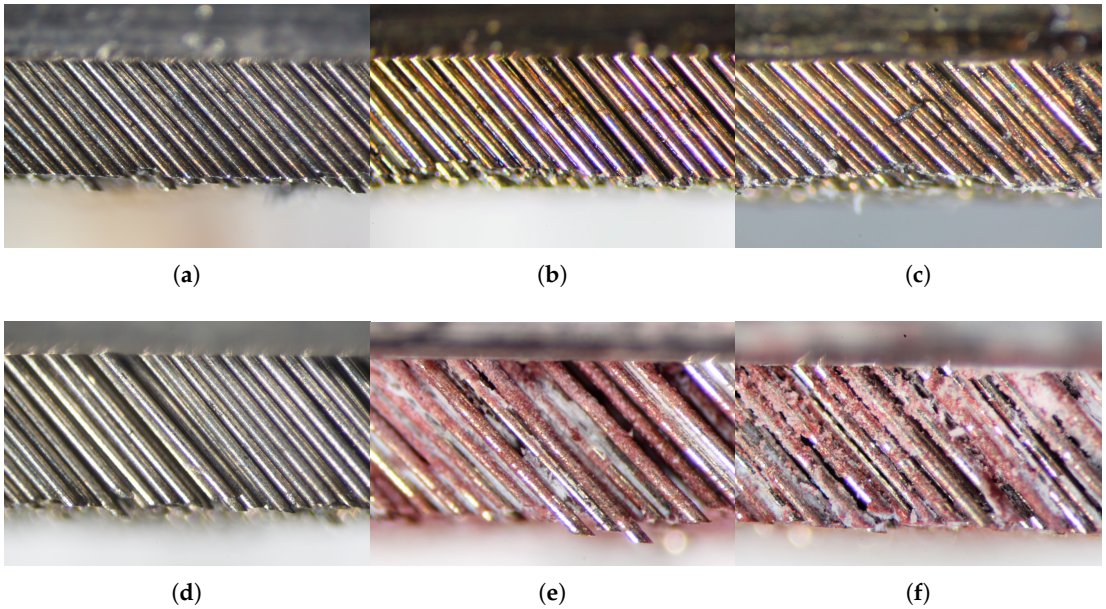

(**a**) (**b**) (**c**)

(**d**) (**e**) (**f**)

Figure 3. (**a**) Microscope image of seal *O* before treatment, (**b**) microscope image of seal *O* after treatment, (**c**) microscope image of seal *O* after stiffness measurement, (**d**) microscope image of seal *S* before treatment, (**e**) microscope image of seal *S* after treatment, (**f**) microscope image of seal *S* after stiffness measurement; the preparation was carried out by Siemens AG and MAN Energy Solutions SE.

A turbine oil typically used in stationary gas turbines was used to contaminate seal *O*. The oil was burnt in at a temperature of 220 °C for a period of 20 hours. The turbine oil was applied directly on

the bristles with a cannula. After application and before the aging cycle, the bristles were completely wetted with turbine oil. This cycle was repeated three times. The carbonised bristle package is shown in Figure 3b.

A salt mixture of iron oxide, trisodium phosphate and sodium carbonate typically found in steam turbines was used to contaminate seal *S*. The seal was immersed in a salt mixture for approximately 30 minutes and then dried at a temperature of 105 °C for approximately 30 minutes. Red-brown iron oxide and crystallized salt mixture are visible between the wires (see Figure 3e).

2.3.2. Evaluation of the Treatment

In order to quantify the degree of contamination of the bristle packages and to obtain a comparative value for the results of the rub tests, the bristle forces were measured both before and after the treatment. During the measurements, the bristle packages were not pressurized. The force-displacement curves were recorded at four equally spaced circumferential positions. The measurements were repeated several times at each circumferential position. The stamp radius was 140 mm with a stamp width of 40 mm.

The force-displacement curves are shown in Figure 4 (Seal *O*) and Figure 5 (Seal *S*). For a better overview, only the force-displacement curves during pressing of the stamp into the bristle package are shown. Due to the contamination, however, a clear increase in hysteresis could be observed, although it is not shown in the figures. The results are also normalised to the maximum force measured in the uncontaminated state. The maximum force occurred for both seals when the maximum interference of approximately 0.85 mm was reached. After each immersion of the stamp, the bristles do not reach their original orientation. Accordingly, the force increase of a subsequent measurement takes place at a further displacement of the stamp. This was corrected by adjusting the initial values.

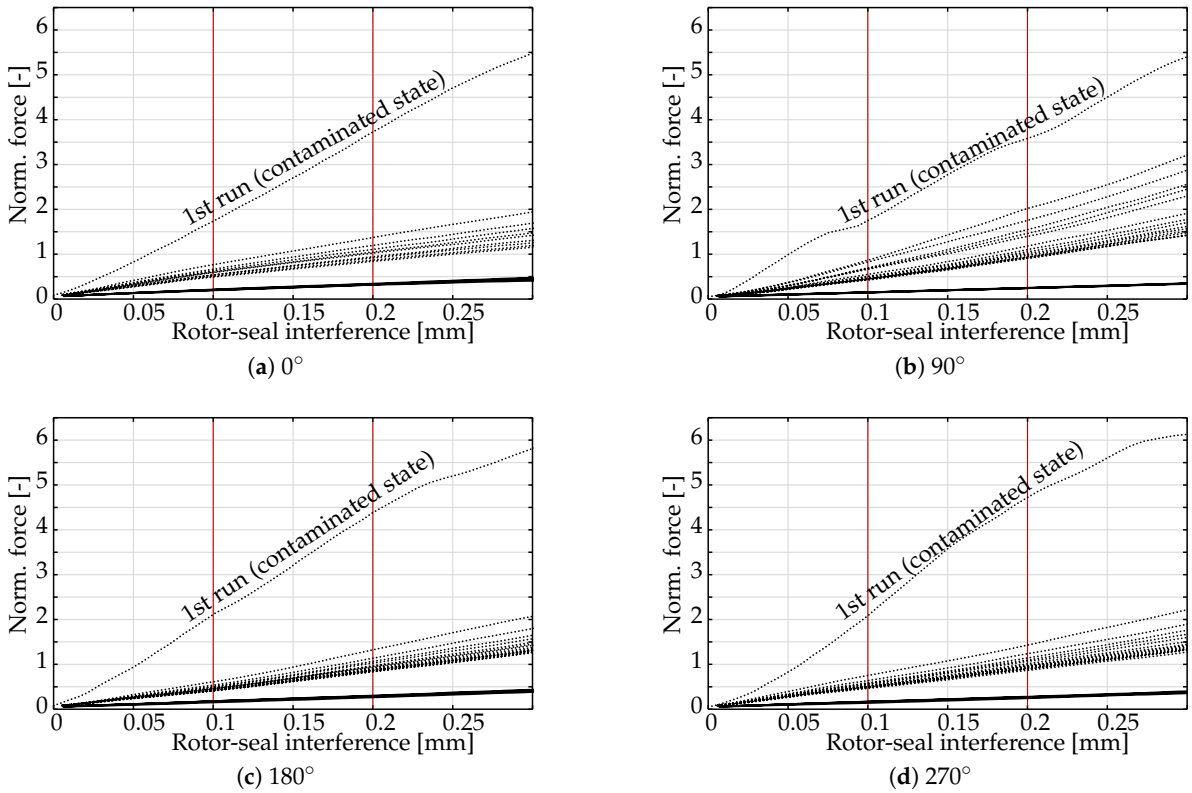

Figure 4. Normalised stamping force over rotor–seal interference for seal *O* at four circumferential positions before (▬) and after the treatment (• • • •); the measurements were carried out by MTU Aero Engines AG.

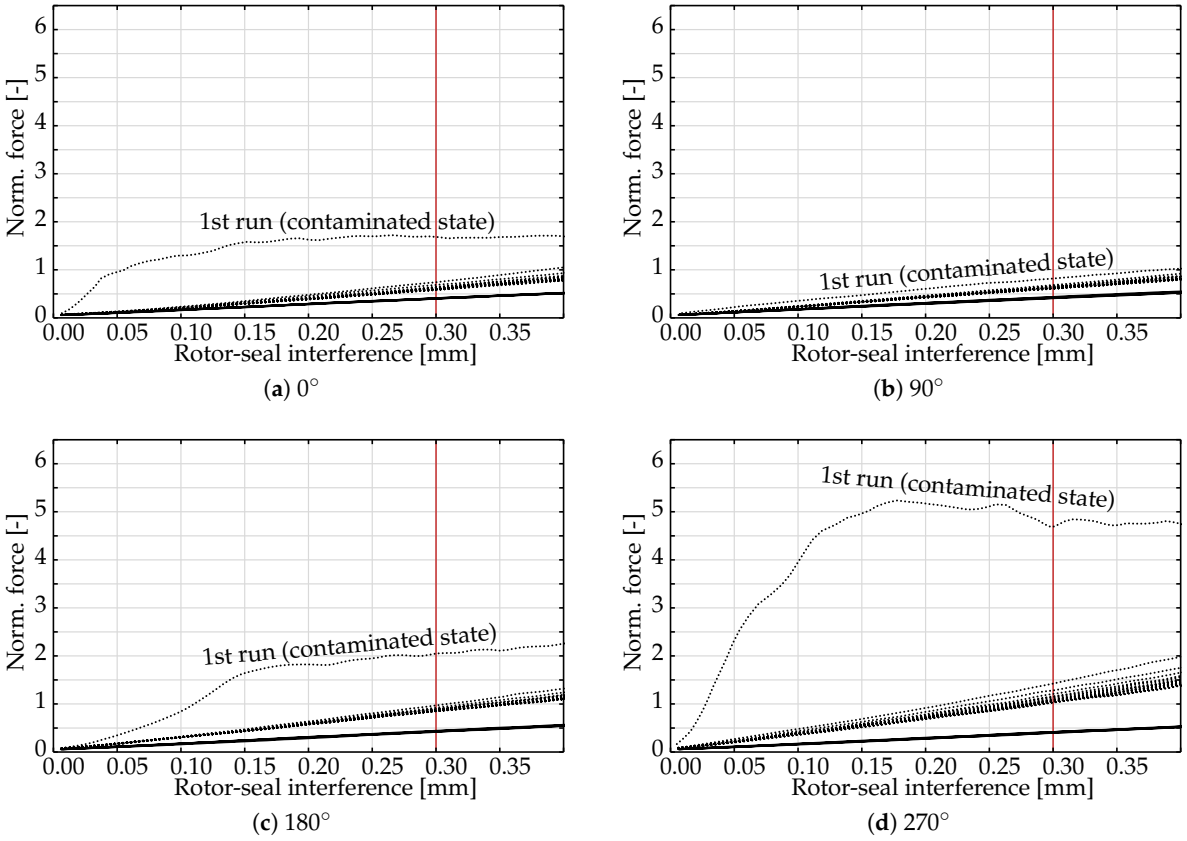

Figure 5. Normalised stamping force over rotor–seal interference for seal *S* at four circumferential positions before (—) and after the treatment (••••); the measurements were carried out by MTU Aero Engines AG.

In the case of both seal *O* and seal *S*, there is a significant increase in the bristle forces during the first immersion of the stamp into the bristle package compared to the uncontaminated state. The different courses of both seals are of interest. While the forces in the case of seal *O* increase continuously up to an interference of approximately 0.5 mm, the forces in the case of seal *S* reach a plateau already after approximately 0.15 mm and do not increase any more or only slightly. This can be explained very well with a cracking of the salt crust. Figure 3f shows the bristle pack at a circumferential positions where the stamp was already immersed in the bristle pack. There is no optical change for seal *O* (see Figure 3c). Nevertheless, in both cases, the bristle forces in the subsequent runs decrease significantly. During measurements with seal *S*, a very large variation of the forces over the circumference can also be observed in the first runs. It probably results from the non-uniform thickness of the salt layer.

The points marked by vertical lines correspond to the rotor–seal interferences set in the rub tests (0.1 and 0.2 for seal *O* and 0.3 mm for seal *S*). Table 2 summarizes the ratios of the bristle forces of the contaminated to the uncontaminated condition.

Table 2. Ratio of normalised bristle force of the contaminated package in relation to the uncontaminated state. Deviations around the circumference are denoted accordingly.

Run	Seal O (0.1 mm Interference)	Seal O (0.2 mm Interference)	Seal S (0.3 mm Interference)
1	11.26 ± 1.19	14.61 ± 1.65	5.66 ± 3.54
2	4.30 ± 0.54	5.43 ± 0.93	2.33 ± 0.71
3	3.80 ± 0.62	4.70 ± 0.89	2.17 ± 0.61
4	3.46 ±0.44	4.30 ± 0.69	2.07 ± 0.56
5	3.36 ± 0.42	4.07 ± 0.65	2.03 ± 0.52
6	3.31 ± 0.48	3.93 ± 0.63	1.99 ± 0.52
7	2.94 ± 0.20	3.61 ± 0.37	1.96 ± 0.51
8	2.86 ± 0.18	3.47 ± 0.28	1.94 ± 0.47
9	2.79 ± 0.17	3.36 ± 0.27	1.94 ± 0.48
10	2.69 ± 0.18	3.26 ± 0.26	1.92 ± 0.47
11	2.60 ± 0.18	3.23 ± 0.17	2.06 ± 0.46
12	2.60 ± 0.16	3.20 ± 0.09	2.06 ± 0.46
13	2.57 ± 0.16	3.14 ± 0.11	2.03 ± 0.44
14	2.52 ± 0.20	3.08 ± 0.11	2.02 ± 0.44
15	2.52 ± 0.12	3.06 ± 0.11	2.04 ± 0.46

2.4. Test Parameters

In order to assess the influence of contamination, measurements of the same seals in their uncontaminated states are used as a reference. These were carried out as part of a previous measurement campaign. In this measurement campaign, rub tests were carried out with variation of the interference between rotor and bristle package, the differential pressure and the circumferential speed. These tests had a scope of 75 (seal *O*) or 28 (seal *S*) rubbing tests. In this paper, however, only the measured values from these test series are used, in which the test parameters correspond to those of the tests in the contaminated state.

When carrying out a rub test with brush seals, it is of vital importance to ensure that the initial positions prior of each rub test are as equal as possible. This is true in particular for the bristle package. On the one hand, the exact knowledge of the current seal and rotor diameter, corresponding to the current state of wear, is required, on the other hand, the package must be brought to a state, which is as unaffected as possible by the previous rub test. The former condition is achieved by measuring the inner diameter of the bristle package after each parameter variation (differential pressure, speed or interference), i.e., after no more than 4–5 rubbing cycles, using a 2D profile laser scanner. Using the diameter measurements, the wear is interpolated linearly and is associated with the respective rub test. When installed in the rig, the bristles are "loosened" after the first rub test with a rod to separate potentially stuck or welded bristles. In addition, an automated process is applied using pressure shocks to minimize hysteretic effects. For further details about actual single rub tests, see [7,8].

In order to investigate the influence of contamination on the rubbing and leakage behaviour, several rub tests were carried out under constant operating conditions. A variation of the operating parameters would have made it more difficult to draw conclusions about the causes of the changes in the measurement data, as both the operating parameters and the stiffness of the bristle package would have changed after each test run.

With the seal *O*, 8 tests were therefore initially carried out with an interference of 0.1 mm, a differential pressure of 3.5 bar and a circumferential speed of 80 m/s. Subsequently, the interference was increased to 0.2 mm and 8 more measurements were carried out. In the case of seal *S*, 16 repeat measurements were carried out with an interference of 0.3 mm and otherwise identical boundary conditions. The duration of the rubbing was 30 s in all tests. Both before and after rubbing, a dwell time of 120 s each was provided, during which all quantities could settle to steady state. The actual rubbing therefore does not differ from the tests in the uncontaminated state. Only the procedures for restoring the same initial state, such as passing through the bristle package with a solid object and

the subsequent application of pressure shocks, were not applied. On the one hand, there was the risk that the contamination layer would be damaged and on the other hand, a sequence of tests that was as uninfluenced as possible was most likely to represent the events in a real machine. In order to further increase the transferability to the real application, wear compensation, as described above, was deliberately omitted. Thus, always the same axial rotor position was approached. In addition, this procedure enables a statement to be made about the change in package flexibility between the tests, such as the blow-down and hysteresis behaviour, provided that the wear is neglected in the first approximation.

The measurements in the contaminated state were carried out with a second uncoated rotor made of Inconel 718 that was identical in design to the one used in the uncontaminated tests. This rotor has already been used for rub tests with brush seals with Kevlar fibre packages. Before the start of the measurements presented in this paper, the rotor showed no measurable wear.

3. Results and Discussion

The following chapter discusses the experimental results of the rub test, starting with the salted seal *S*.

3.1. Generation and Distribution of Rubbing Heat

The total frictional power loss is obtained by subtracting the motor power during rubbing from the power before rubbing. The rotational speed remains almost constant during a rub test. However, a slight reduction in speed at the beginning of the rubbing could not be completely avoided. The total power loss was corrected accordingly by adding the power to decelerate the rotor and subtracting the power to accelerate the rotor to the initial value. The heat flux distribution is obtained as the ratio of rotor heat input calculated by means of the finite element analysis and the measured total frictional power loss:

$$heat\ flux\ distribution = \frac{rotor\ heat\ input}{total\ frictional\ power\ loss}. \quad (3)$$

In Table 3, the measurement accuracies are listed.

Table 3. Measurement and repeat accuracies.

Parameter			
pressure difference	(mbar)	±62.15	**Measurement**
total frictional power loss	(-)	±0.123%	**accuracies**
rotor–seal interference	(mm)	±0.019	**Repeat accuracies**

3.2. Results Seal S

Figure 6a shows the normalised total friction power losses and normalised rotor heat inputs, as well as the ratio of the two to each other, for all 16 rubbing tests. The values are averaged over the total rubbing time of 30 s each. In order to ensure comparability of the results, the values were normalized to the starting value of seal 2 at 0.1 mm (see the authors' previous publication [22], Figure 4). As expected, both the total power loss and the rotor heat input decrease with continuous testing. This can be explained on the one hand by progressive seal and rotor wear and on the other hand by a presumably deteriorated hysteresis behaviour of the seal due to contamination. Both causes a reduction of the actual interference between the rotor and the bristle package.

Furthermore, two phenomena are noticeable:

1. The total power loss and the rotor heat input increase until the second repeat measurement.
2. This increase can be observed again every fourth measurement.

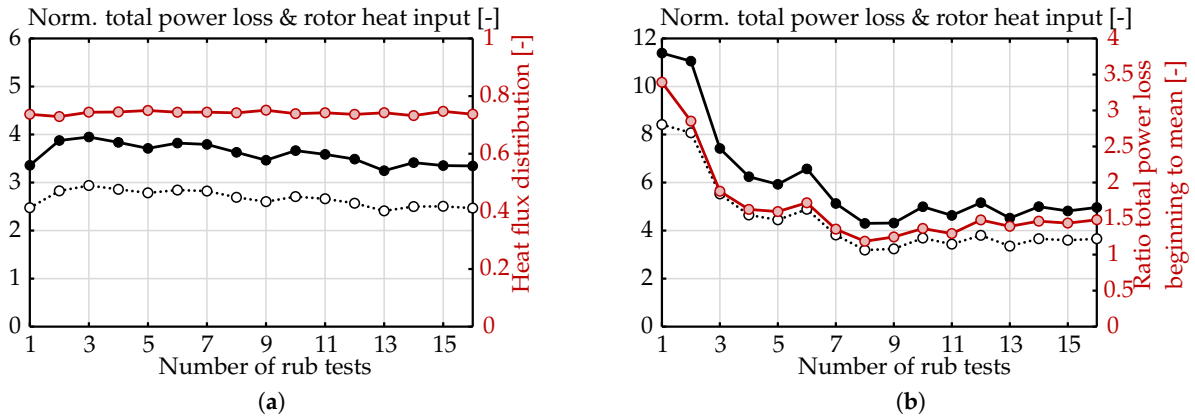

Figure 6. (**a**) Normalised total power loss (—●—), rotor heat input (• ○ •) and heat flux distribution (—○—); the results shown represent values averaged over the rubbing duration. (**b**) Normalised total power loss (—●—), rotor heat input (• ○ •) and ratio of total power loss at the beginning to averaged value (—○—); the shown power losses and heat inputs represent values at the beginning of rubbing.

Figure 6b explains the first observation. The normalised total power losses and the normalised rotor heat inputs are shown as starting values at the beginning of the rubbing process. In addition, the ratio of the initial values of the total power losses to the averaged values is shown. On the basis of the values shown, a sharp increase in the friction power at the beginning of the first rubbing processes can be seen. In the first two runs in particular, a frictional power increase of approximately a factor of 3 in relation to the mean value is observed. The additional force required to break the salt crust on the bristle package is responsible for the higher values (see Figure 3f). As soon as this resistance is overcome, the frictional power loss decreases strongly over the time the bristle is rubbed, as the bristle package remains in this position after deflection (see also later consideration of the hysteresis behaviour (see Figure 8). In the following repeat measurements, no such strong rubbing is observed at the beginning, since the salt crust has already been broken up. The hysteresis behaviour, i.e., the mobility of the bristle pack, also improves steadily. The initial values thus approach the mean value. Overall, a change in the course of the frictional power loss is more likely to be observed during the rubbing process itself rather than an effect on the mean values. However, since the drops were so severe, especially during the first run, the mean value also rises slightly. The repetition of the increase after every fourth measurement is related to the fact that after four runs, a measurement of the seal's inner diameter was carried out. The seal was not removed from the test rig during this process. Meanwhile, there was a short interruption of approximately 45 minutes between the rub tests. During this time, it is conceivable that the package has settled again somewhat or that the housing or the rotor have cooled down to different degrees.

If the results of the tests on the contaminated seal are compared with the measurements of the same seal in the uncontaminated state, it can be seen that both the average total power losses and the rotor heat inputs have increased only minimally and, after approximately 10 runs, reach approximately the values of the uncontaminated seal (norm. total power loss 3.65 ± 0.15 / norm. rotor heat input 2.39 ± 0.24). The same applies to the ratio of the total power loss at the beginning to the mean value, which was 1.39 ± 0.12 in the previous measurements. Only the heat flux distribution is higher compared to the rub tests in the uncontaminated state (65.35 ± 0.10 %). One reason for this could be a lower leakage flow through the bristle package due to contamination and thus a lower convective heat transfer from the bristles, but also combined with the effect of insulation as a result of contamination. Furthermore, two rotors identical in design were used in the tests. Manufacturing accuracies, in particular with regard to the temperature measuring positions, can therefore play a role, albeit of secondary importance.

The conclusions drawn so far can also be understood from the temperature curves. Figure 7a shows the maximum temperatures in the friction contact between rotor and bristle package as well as the maximum measured rotor temperatures. The first value is a calculated quantity derived from the FE Analysis. In both cases, there is a continuous decrease in the maximum temperatures. After 13 runs, the temperatures almost reach the level of the uncontaminated seal (540 $\pm$ 1 K/426 $\pm$ 10 K). Figure 7b shows the temperature curves of the rotor thermocouple which is located closest to the contact point and thus records the highest temperatures. For a better overview, only every second run is shown. As can be seen in Figure 7b, the highest temperatures were measured after a few seconds of rubbing, with an even greater drop towards the end of the rubbing period, especially in the first run. In the following runs, both the maximum temperatures decrease and the time until these temperatures are reached shifts further and further towards the end of the run.

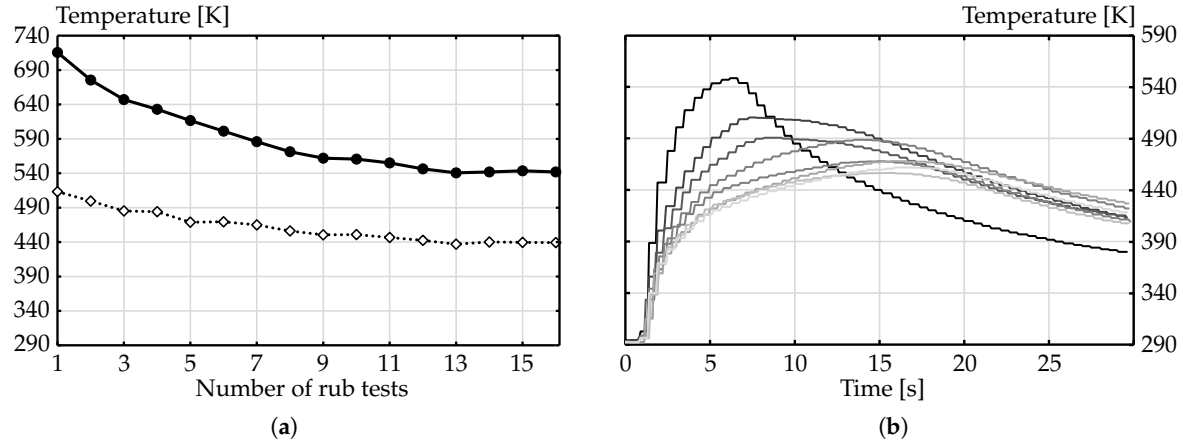

Figure 7. (**a**) Maximum temperature in the contact zone between seal and rotor (value out of FEA) (—●—) and maximum rotor temperature (•◇•). (**b**) Course of the maximum rotor temperature over the rubbing duration, first run (——) to last run (——).

It could already be deduced from the results shown so far that the hysteresis behaviour of the seal must have deteriorated due to contamination. Figure 8 shows the discharge coefficients as the mean values for the time periods before, during and after rubbing for all 16 runs.

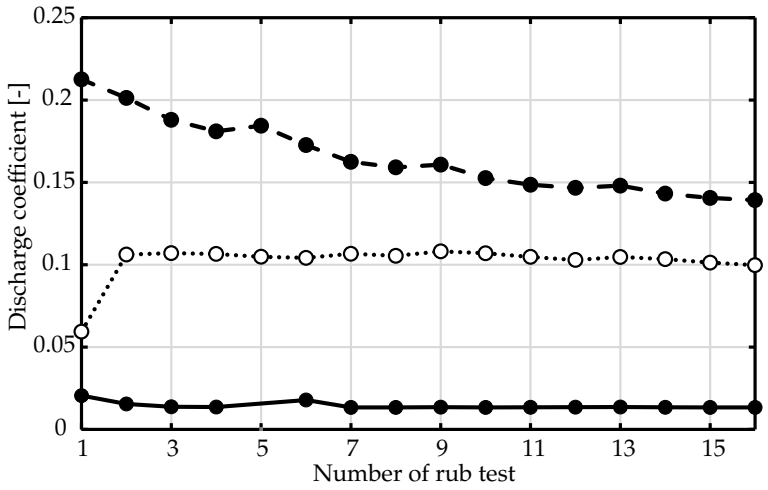

Figure 8. Discharge coefficients for the states before (•○•), during (—●—) and after (-●-) rubbing.

Looking at the course of the discharge coefficient before rubbing, it can be seen that a value of 0.058 is obtained before the first rubbing. This corresponds approximately to the value of the rub tests in the uncontaminated state (0.05 $\pm$ 0.002) and shows that a comparable initial state has been established.

During the rubbing process, the sealing effect improves and the discharge coefficient decreases. After the first rubbing, the discharge coefficient rises to almost 0.21. This represents a significant deterioration of the hysteresis behaviour compared to the uncontaminated state (0.119 ± 0.003). Due to the fact that no measures have been taken to improve reproducibility, such as the application of pressure shocks, the bristle package remains in a deflected position and the discharge coefficient before the second rubbing is significantly increased. However, the hysteresis behaviour improves continuously, as can be seen from the decrease in the discharge coefficient after rubbing. This is most likely due to a detachment of the salt crust from the bristle package (see Figure 9d,e). It is interesting to note that the leakage before rubbing does not change significantly after the first measurement.

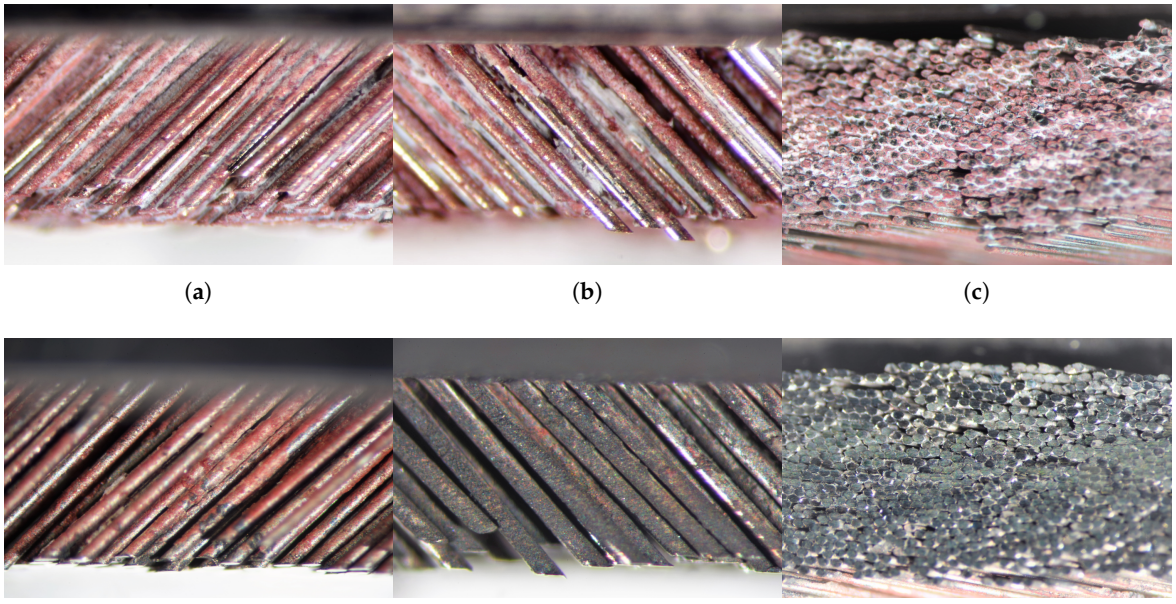

Figure 9. (**a**) Microscope image of seal *S* front plate side before experiments, (**b**) microscope image of seal *S* back plate side before experiments, (**c**) microscope image of the underside of bristle package of seal *S* before experiments, (**d**) microscope image of seal *S* front plate side after experiments, (**e**) microscope image of seal *S* back plate side after experiments, (**f**) microscope image of the underside of bristle package of seal *S* after experiments.

After all measurements had been completed, the seal *S* was examined more closely under the microscope. Figure 9a–c shows the initial conditions before the start of the rub tests. Figure 9d–f shows the corresponding images after all measurements have been completed. The salt crust on both the upstream and downstream bristles has almost completely disappeared. No agglutinated bristles could be found on the photos. Only a coating of red iron oxide can still be seen on the upstream side. On the side of the back plate, additional abrasion of the rotor and sealing material was deposited and the layer of iron oxide was covered. On the underside of the package, the contamination layer has also been completely removed.

3.3. Results Seal O

The following chapter discusses the experimental results of the rub tests of the carbonised seal *O*. The test series is divided into two sections. Firstly, eight consecutive rubbing tests were carried out with a small overlap. Subsequently, a further series of eight rubbing tests was carried out with an interference of 0.2 mm. There was no removal of the seal or an application of the measures to increase reproducibility (pressure shocks or similar) between the tests.

Prior to the first rub tests, the bristle package was already brought to an interference of 0.1 mm without rotation. This was done to prevent a too high heat input due to an extremely stiff bristle package after the treatment with oil. Figure 10a shows the results in the form of normalised total power loss and normalised rotor heat input, as well as the ratio of the two to each other. The values are averaged over the entire rubbing time of 30 s each.

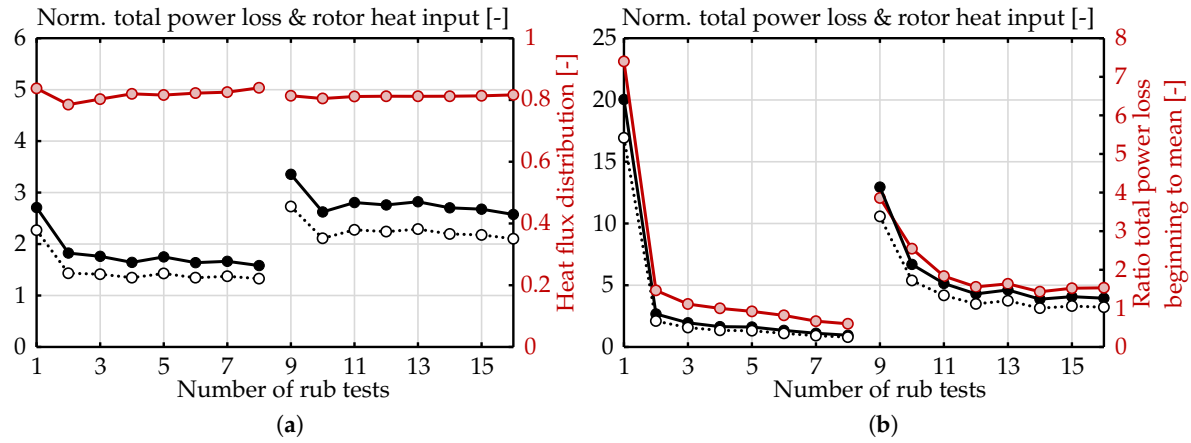

Figure 10. (**a**) Normalised total power loss (●), rotor heat input (○) and heat flux distribution (●); the results shown represent values averaged over the rubbing duration. (**b**) Normalised total power loss (●), rotor heat input (○) and ratio of total power loss at the beginning to averaged value (●); the shown power losses and heat inputs represent values at the beginning of the rubbing duration.

In contrast to the salted seal *S*, contamination of the seal *O* has a strong effect on the mean values of the first passes. The reason for this lies in the extreme total power losses and rotor heat inputs at the beginning of the rubbing process (see Figure 10b), which occur despite the previous compression of the package without rotation. In these cases, the total power losses collapse significantly after a few seconds, as can be derived from the ratios of the total power losses at the beginning of the rubbing process to the respective mean value of more than 7 or approximately 4. Nevertheless, a higher average value is obtained over the rubbing time of 30 s. The collapse occurs because the package remains in its radially deflected position after overcoming the spring return forces of the bristles and the additional resistance due to contamination. The contamination in combination with the friction between the bristles and on the back plate prevents the bristles from returning completely to their initial position even after completion of the rubbing process. After the first runs of each interference stage, the average values of the total power loss and rotor heat input remain at a similarly lower level. Due to the fact that the bristles do not return completely, the actual interference after the first rubbing process is lower. Only the initial values decrease further, similar to seal *S*, as the flexibility of the package increases.

The rubbing processes at an interference of 0.2 mm cannot be considered separately from the previous tests. As a result, the frictional forces at the beginning of the rubbing are lower than for the first measurement with lower interference.

A comparison with the results of the same seal in its uncontaminated state is also interesting. As expected, the mean total power losses of the first runs of each interference level achieved higher values than in the uncontaminated state. In the uncontaminated state, the following mean values were obtained: norm. total power loss 0.1 mm: 2.33 $\pm$ 0.19 and 0.2 mm: 2.84 $\pm$ 0.27/norm. rotor heat input 0.1 mm: 1.33 $\pm$ 0.22 and 0.2 mm: 1.82 $\pm$ 0.27. In the case of the lower interference of 0.1 mm, however, all the values of the mean total power loss from the 2nd run onwards are significantly lower. As described above, this is due to the lower actual interference ratio. In the case of the higher interference of 0.2 mm, a similar level of the mean total power loss is achieved in comparison to the results in the uncontaminated state. Of particular interest is the significantly higher heat flux

distribution compared to the measurements in the uncontaminated state (0.1 mm: 56.5 ± 4.9 % and 0.2 mm: 64.9 ± 2.6 %). The leakage mass flows are slightly higher or lower than in the comparative measurements, depending on the run. These differences, therefore, are not relevant. However, it is conceivable that a reduced convective heat transfer from the bristles could be responsible. It could be significantly reduced by the contamination, which acts as a kind of insulation.

The knowledge gained can also be verified on the basis of temperature curves. Figure 11a shows both the maximum rotor temperatures in friction contact originating from the FE analysis and the measured maximum rotor temperatures. The maximum temperatures represent the highest values measured to date on the ITS brush seal test rig. The following values were measured in the uncontaminated condition: Maximum temperature in friction contact at 0.1 mm interference: 474 ± 20 K and at 0.2 mm interference: 538 ± 23 K; maximum rotor temperature at 0.1 mm interference: 384 ± 18 K and at 0.2 mm interference: 413 ± 9 K.

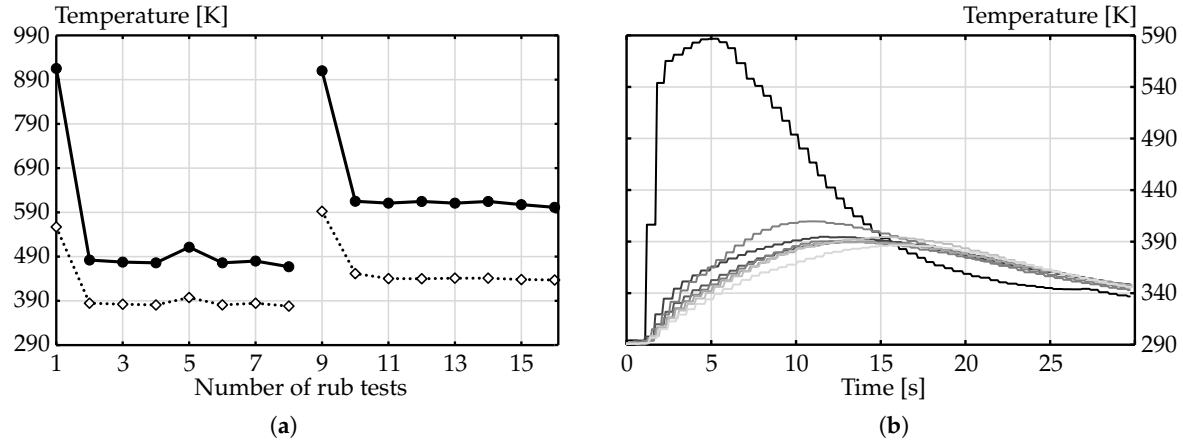

Figure 11. (**a**) Maximum temperature in the contact zone between seal and rotor (value out of FEA) (—●—) and maximum rotor temperature (•◇•). (**b**) Course of the maximum rotor temperature over the rubbing duration, first run (—) to last run (—).

Figure 11b shows the time-dependent temperature curves of the first eight rub tests. The thermocouple which was closest to the contact point was selected. The temperature increase at the beginning of the rub test and the sharp drop that follows are even more pronounced than with the salted seal *S*. In contrast to the salted seal, all subsequent courses no longer differ significantly from each other.

Figure 12 shows the leakage rates through the seal for the conditions before, during and after rubbing based on the discharge coefficients. A discharge coefficient of approximately 0.079 is achieved before the first rubbing, which is very close to the value of the seal in the uncontaminated state (0.071 ± 0.0017), i.e., comparable conditions are given. After the first rubbing, the discharge coefficient increases to 0.193, which is clearly above the comparative value of 0.148 ± 0.005. It is particularly interesting that the bristle package remains almost in this deflected position. The following differences between the states before and after the rubbing are therefore minimal. Due to the contamination, the seal shows almost no recovery behaviour.

While the series of tests considered in Figure 12 were carried out without the application of pressure shocks between the individual rubbing processes, no significant improvement could be achieved with a later test application of up to 36 pressure shocks.

Figure 12 shows that the states described above do not change even for a higher interference of 0.2 mm. The discharge coefficients now increase after the first rub event due to the further radially deflected bristle package.

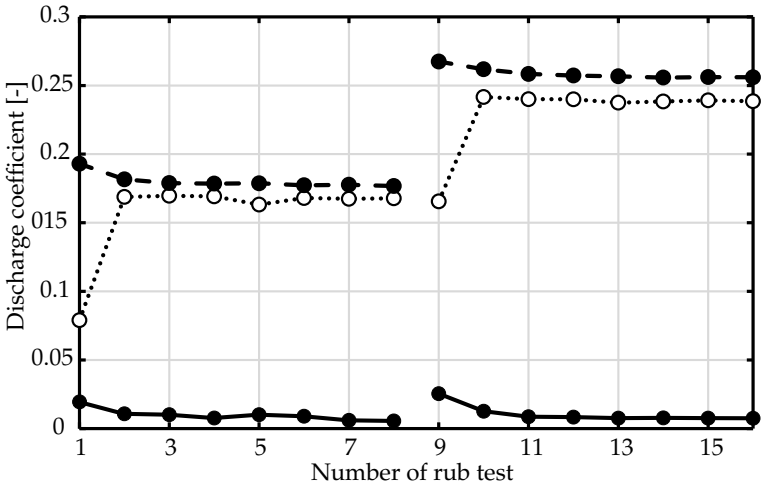

Figure 12. Discharge coefficients for the states before (• ○ •), during (—●—) and after (-●-) rubbing.

The package images for the time points before and after the experiments are compared in Figure 13a–f. On the upstream side of the bristles, the oil layer has almost disappeared. Occasionally, black coked remains of the oil are visible. On the downstream side below the support ring, however, a clear accumulation of coked material can be found. An exact material analysis is not possible within the scope of the research study. Due to the consistency, however, it can be assumed that it is largely a mixture of coked oil and metallic material removal from the bristles and rotor. On the underside of the package, clear traces of rubbing and "smearing" of the bristle tips can be seen after the tests. However, this could also be found in the unpolluted state of this seal after rubbing. After completion of the measurements, the package was not passed through with a solid object in order to separate the bristles from each other. However, this happened before the preparation, which is why the rub marks are not visible in the image Figure 13c.

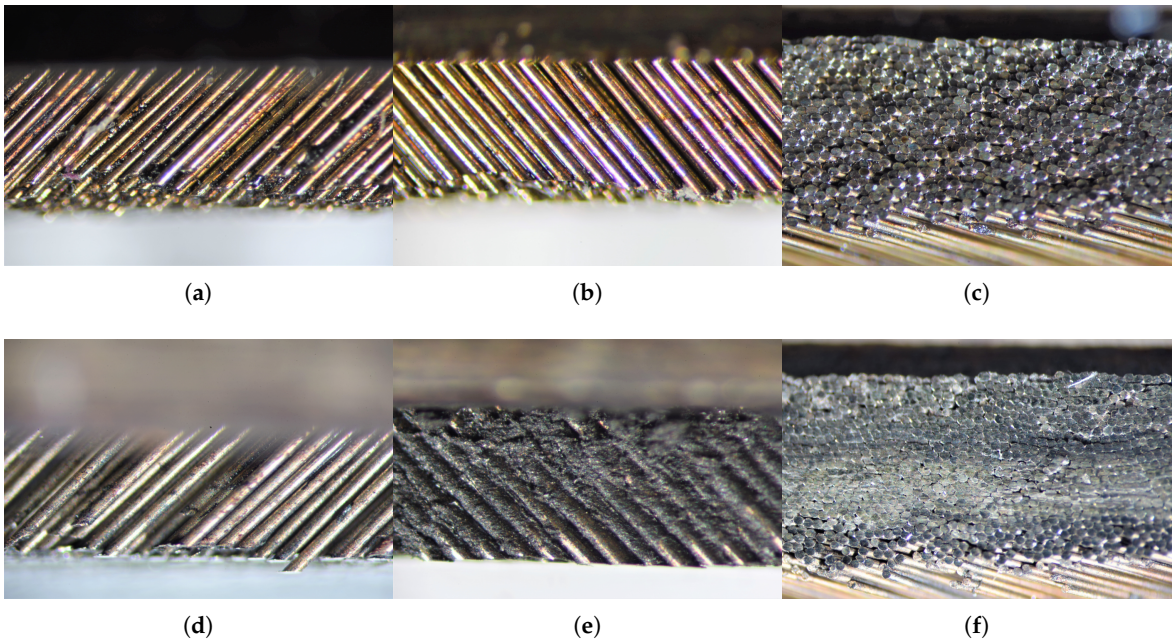

Figure 13. (**a**) Microscope image of seal *O* front plate side before experiments, (**b**) microscope image of seal *O* back plate side before experiments, (**c**) microscope image of the underside of bristle package of seal *O* before experiments, (**d**) microscope image of seal *O* front plate side after experiments, (**e**) microscope image of seal *O* back plate side after experiments, (**f**) microscope image of the underside of bristle package of seal *O* after experiments.

3.4. Comparison of Stamp Measurement and Rub Tests

After completion of the rubbing tests and the availability of the resulting data, a comparison with the previously measured force-displacement curves is possible. In Figure 14a–c, the total power losses normalised to the maximum value at the beginning of the rubbing and the corresponding stamp forces at the corresponding interference are plotted. The stamp forces are normalised with the stamp force of the first run. In the case of seal *O*, only the gradients can be compared with each other in general. On the one hand, this is due to the fact that seal *O* was already brought to an interference of 0.1 mm before the first rub test without rotation and on the other hand, because the later tests with the interference of 0.2 mm must not be considered separately from the previously carried out tests. In terms of quality, there is quite good agreement between the decrease in frictional power and the decrease in stamp force in subsequent measurements.

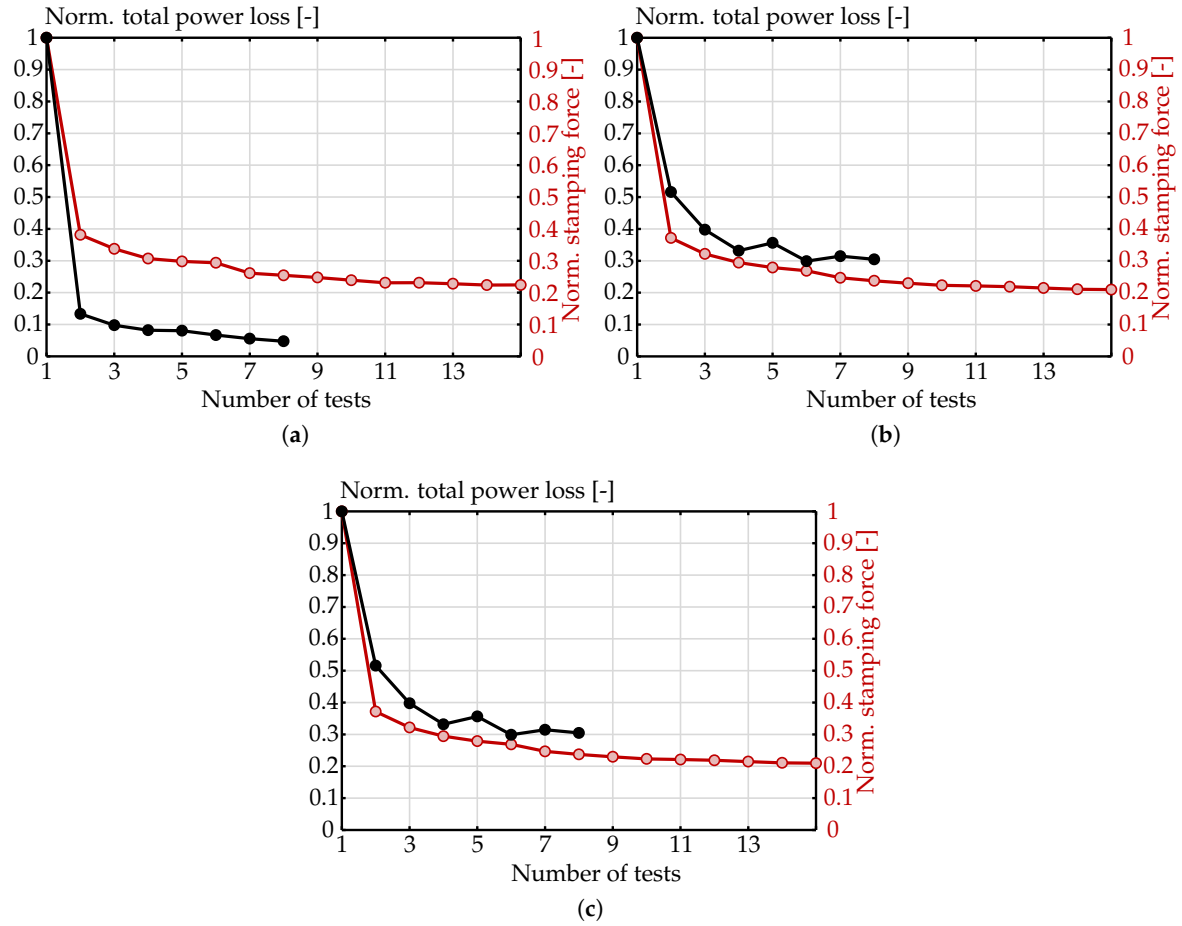

Figure 14. Normalised total power loss at the beginning of the rub test (—●—) and normalised stamping force (—○—). (**a**) Seal *O* and rotor–seal interference of 0.1 mm, (**b**) seal *O* and rotor–seal interference of 0.2 mm, (**c**) seal *S* and rotor–seal interference of 0.3 mm.

In the case of seal *S*, a direct comparison is possible (see Figure 14c). Compared to the normalised total power losses, the stamp forces drop considerably after the first test run and reach a constant final value after less tests. An estimate of the total power loss to be expected at the beginning of the rub test based on the measured data of the rub tests in the uncontaminated state and with the aid of the force-displacement measurements after preparation is nevertheless possible and reasonable.

4. Conclusions

In an experimental test campaign at ITS, the influence of the degree of contamination on the rubbing and leakage behaviour of brush seals was investigated. For this purpose, two seals that had already been tested in a new condition were specifically prepared with oil and salt. In each case, a series of rub tests with constant boundary conditions were carried out. Due to the significantly increased package stiffnesses as a result of the contamination, very high frictional power losses and heat inputs resulted, especially at the beginning of the rubbing processes. For the salted seal, however, there were no significant changes in the average frictional power losses and rotor heat inputs over the entire rubbing period of 30 s, as these dropped after the additional bristle forces had been overcome and the package remained in its deflected position due to friction. This behaviour was also observed in the case of the carbonised seal. Here, however, the initial frictional power losses were so high that an influence on the averaged frictional power losses was given.

The hysteresis behaviour deteriorated as expected due to the contamination. In the case of the salted seal, however, a continuous improvement of the leakage performance could be observed, since parts of the salt crust were loosened again in the course of the measurements. In the case of the carbonised seal, there was no significant improvement in the leakage performance.

The heat flux distribution was higher in the rub tests compared to the uncontaminated condition. In the case of the salted seal, an increase of approximately 13.3 % was quantified. In the case of the carbonised seal, an increase of approximately 25.1 to 44.8 % was determined, depending on the interference level. The reason could be the layer of contamination on the bristles acting as insulation and therefore reducing the convective heat transfer.

Author Contributions: Conceptualization, M.H.; Methodology, M.H.; Formal analysis, M.H.; Investigation, M.H.; Resources, C.S. and H.-J.B.; Writing—original draft preparation, M.H.; Writing—review and editing, C.S. and H.-J.B.; Supervision, C.S. and H.-J.B.; Project administration, M.H., C.S. and H.-J.B.; Funding acquisition,M.H., C.S. and H.-J.B.

Funding: This research was funded by FVV ("Forschungsvereinigung Verbrennungskraftmaschinen e.V."), project number 1255. The APC was funded by Deutsche Forschungsgemeinschaft and Open Access Publishing Fund of Karlsruhe Institute of Technology.

Acknowledgments: The investigations in this scientific publication are the result of a research project, which has been initiated by the FVV ("Forschungsvereinigung Verbrennungskraftmaschinen e.V.") and carried out at the Institute of Thermal Turbomachinery, Karlsruhe Institute of Technology. The work has been supported financially by the FVV and the participating companies. This support is gratefully acknowledged. Special thanks go to Joris Versluis (MTU Aero Engines), who served as project chair and coordinated important technical communication between all partners. We acknowledge support by Deutsche Forschungsgemeinschaft and Open Access Publishing Fund of Karlsruhe Institute of Technology

Conflicts of Interest: The authors declare no conflict of interest. The founding sponsors had no role in the design of the study; in the collection, analyses, or interpretation of data; in the writing of the manuscript, and in the decision to publish the results.

Abbreviations

The following abbreviations are used in this manuscript:

A	Gap area between back plate and rotor
b	Bristle pack width
c_d	Discharge coefficient
d_b	Bristle diameter
d_B	Bore hole diameter
d_s	Seal inner diameter
h	Heat transfer coefficient
$\dot{m}_\mathrm{bs}$	Mass flow through brush seal
$\dot{m}_\mathrm{ideal}$	Idealized, inviscid gap flow
p	Pressure

R	Specific gas constant
r_{TC}	Radial distance of bore hole to rotor surface
s_{ax}	Axial distance of package to back plate
s_{HI}	Axial position of heat impact
s_{TC}	Depth of the bore hole
T	Temperature
u	Circumferential velocity
Greek Symbols	
κ	Heat capacity ratio
λ	Laying angle
ρ_p	Packing density
Subscripts	
in	Inlet
out	Outlet
t	Total
Abbreviations	
ITS	Institut für Thermische Strömungsmaschinen (engl.: Institute of Thermal Turbomachinery)
FEA	Finite element analysis
KCl	Potassium chloride
NaCl	Sodium chloride
O	Oil
S	Salt
TC	Thermocouple

References

1. Holle, G.F.; Krishnan, M.R. Gas Turbine Engine Brush Seal Applications. In Proceedings of the 26th AIAA/ASME/SAE/ASEE Joint Propulsion Conference & Exhibit, Orlando, FL, USA, 16–18 July 1990; doi:10.2514/6.1990-2142.
2. Mahler, F.; Boyes, E. The Application of Brush Seals in Large Commercial Jet Engines. In Proceedings of the 31st AIAA/ASME/SAE/ASEE Joint Propulsion Conference & Exhibit, San Diego, CA, USA, 10–12 July 1995; doi:10.2514/6.1995-2617.
3. Wolfe, C.E.; Chiu, R.P.; Cromer, R.H.; Crum, G.A.; Marks, P.T.; Stuck, A.E.; Turnquist, N.A.; Reluzco, G.; Dinc, O.S. Brush Seals in Industrial Gas Turbines. In Proceedings of the 33rd AIAA/ASME/SAE/ASEE Joint Propulsion Conference & Exhibit, Seattle, WA, USA, 6–9 July 1997; doi:10.2514/6.1997-2730.
4. Soditus, M.S. Commercial Aircraft Maintenance Experience Relating to Current Engine Seal Technology. In Proceedings of the 34th AIAA/ASME/SAE/ASEE Joint Propulsion Conference & Exhibit, Cleveland, OH, USA, 13–15 July 1998; doi:10.2514/6.1998-3284.
5. Chupp, R.E.; Ghasripoor, F.; Turnquist, N.A.; Demiroglu, M.; Aksit, M.F. Advanced Seals for Industrial Turbine Applications: Dynamic Seal Development. *J. Propul. Power* **2002**, *18*, 1260–1266, doi:10.2514/2.6061.
6. Osterhage, T.; Büscher, S.; Kosyna, G.; Glienicke, J.; Urlichs, K. Multiple Rows Brush Seal Testing for Steam Turbine Applications with High Temperature and High Pressure Conditions and Long Service Intervals. In Proceedings of the 6th European Conference on Turbomachinery, Lille, France, 7–11 March 2005.
7. Hildebrandt, M.; Schwarz, H.; Schwitzke, C.; Bauer, H.J.; Friedrichs, J. Effects of the Back Plate Inner Diameter on the Frictional Heat Input and General Performance of Brush Seals. *Aerospace* **2018**, *5*, 58, doi:10.3390/aerospace5020058.
8. Hildebrandt, M.; Schwitzke, C.; Bauer, H.J. Experimental Investigation on the Influence of Geometrical Parameters on the Frictional Heat Input and Leakage Performance of Brush Seals. *J. Eng. Gas Turbines Power* **2019**, *141*, 042504, doi:10.1115/1.4038767.
9. Demiroglu, M.; Tichy, J.A. An Investigation of Heat Generation Characteristics of Brush Seals. In Proceedings of ASME Turbo Expo 2007: Power for Land, Sea, and Air, Montreal, QC, Canada, 14–17 May 2007; doi:10.1115/GT2007-28043.

10. Ruggiero, E.; Allen, J.; Demiroglu, M.; Lusted, R.M. Heat Generation Characteristics of a Kevlar Fiber Brush Seal. In Proceedings of the 43rd AIAA/ASME/SAE/ASEE Joint Propulsion Conference & Exhibit, Cincinnati, OH, USA, 8–11 July 2007; p. 5738, doi:10.2514/6.2007-5738.
11. Ruggiero, E.; Allen, J.; Lusted, R.M. Heat Generation Characteristics of a Carbon Fiber Brush Seal. In Proceedings of the 44th AIAA/ASME/SAE/ASEE Joint Propulsion Conference & Exhibit, Hartford, CT, USA, 21–23 July 2008; p. 4508, doi:10.2514/6.2008-4508.
12. Flouros, M.; Hendrick, P.; Outirba, B.; Cottier, F.; Proestler, S. Thermal and Flow Phenomena Associated With the Behavior of Brush Seals in Aero Engine Bearing Chambers. *J. Eng. Gas Turbines Power* **2015**, *137*, 092503, doi:10.1115/1.4029711.
13. Huang, S.; Suo, S.; Li, Y.; Wang, Y. Theoretical and Experimental Investigation on Tip Forces and Temperature Distributions of the Brush Seal Coupled Aerodynamic Force. *J. Eng. Gas Turbines Power* **2014**, *136*, 052502, doi:10.1115/1.4026074.
14. Raben, M.; Friedrichs, J.; Flegler, J. Brush Seal Frictional Heat Generation: Test Rig Design and Validation Under Steam Environment. In Proceedings of the ASME Turbo Expo 2016: Turbomachinery Technical Conference and Exposition, Seoul, South Korea, 13–17 June 2016; doi:10.1115/GT2016-56951.
15. Pastrana, R.M.; Wolfe, C.E.; Turnquist, N.A.; Burnett, M.E. Improved Steam Turbine Leakage Control With A Brush Seal Design. In *Proceedings of the 30th Turbomachinery Symposium*; Texas A&M University, Turbomachinery Laboratories: College Station, TX, USA, 2001; doi:10.21423/R1H65W.
16. Golinkin, S.L.; Lipski, M.J.; Conlow, F.J. Modernization of Existing US Navy Steam Turbines: Efficiency, Reliability and Maintainability. In Proceedings of the ASME Turbo Expo 2010: Power for Land, Sea, and Air, Glasgow, UK, 14–18 June 2010; pp. 993–1012, doi:10.1115/GT2010-22472.
17. Aksit, M.; Bhate, N.; Bouchard, C.; Testo-Blakelock, C.; Demiroglu, M. Evaluation of Brush Seal Performance for Oil Sealing Applications. In Proceedings of the 39th AIAA/ASME/SAE/ASEE Joint Propulsion Conference & Exhibit, Huntsville, AL, USA, 20–23 July 2003; p. 4695, doi:10.2514/6.2003-4695.
18. Stephen, D.; Hogg, S.I. Development of Brush Seal Technology for Steam Turbine Retrofit Applications. In Proceedings of the International Joint Power Generation Conference collocated with TurboExpo 2003, Atlanta, GA, USA, 16–19 June 2003; pp. 505–512, doi:10.1115/IJPGC2003-40103.
19. Neef, M.; Sulda, E.; Surken, N.; Walkenhorst, J. Design Features and Performance Details of Brush Seals for Turbine Applications. In Proceedings of the ASME Turbo Expo 2006: Power for Land, Sea, and Air, Barcelona, Spain, 8–11 May 2006; pp. 1385–1392, doi:10.1115/GT2006-90404.
20. Samudrala, O.; Wolfe, C.E.; Kumar, S.; Chupp, R.E. Design optimization of a retractable holder for compressor discharge brush seal. In Proceedings of the ASME 2011 Turbo Expo: Turbine Technical Conference and Exposition, Vancouver, BC, Canada, 6–10 June 2011; pp. 845–857, doi:10.1115/GT2011-45756.
21. Cardone, G.; Astarita, T.; Carlomagno, G. Heat Transfer Measurements on a Rotating Disk. *Int. J. Rotat. Mach.* **1997**, *3*, 1–9, doi:10.1155/S1023621X97000018.
22. Hildebrandt, M.; Schwitzke, C.; Bauer, H.-J. Experimental Investigation on the Influence of Geometrical Parameters on the Frictional Heat Input and Leakage Performance of Brush Seals. In Proceedings of the ASME Turbo Expo 2017: Turbomachinery Technical Conference and Exposition, Charlotte, NC, USA, 26–30 June 2017; doi:10.1115/GT2017-63423.